The coupling between brain connectivity and heartbeat dynamics unveils the altered interoceptive mechanisms in Parkinson's disease

Diego Candia-Rivera*, Marie Vidailhet, Mario Chavez, and Fabrizio de Vico Fallani.
Sorbonne Université, Paris Brain Institute (ICM), INRIA, CNRS, INSERM, AP-HP, Hôpital Pitié-Salpêtrière Paris, France
** Correspondence: diego.candiarivera@icm-institute.org*

Abstract

Parkinson's disease (PD) is often known for its classical motor symptoms, but non-motor symptoms are often reported including interoceptive and autonomic dysfunctions. Autonomic dysfunctions, such as cardiovascular, urinary, or thermoregulatory abnormalities, are more prone to be associated with motor and cognitive decline, as well as increase the risk of mortality. More recent evidence has shown that Parkinsonian patients may experience alterations in interoceptive processing, i.e., reduced sensitivity to accurately sensing and interpreting internal cues, leading to further impairment in self-awareness, cognitive and emotional processing. Noteworthy, the mechanisms behind these autonomic/interoceptive dysfunctions are not well understood. During the early stages of PD, disruptions in the connectivity of multiple brain regions occur, which has prompted the study of PD as a network-level phenomenon. Our hypothesis is that by examining the relationship between brain connectivity and heartbeat dynamics, we can gain insight into the large-scale network disruptions and the neurophysiology of the disrupted interoceptive mechanisms in PD. Our results show that the coupling of fluctuating alpha and gamma connectivity with heartbeat dynamics is reduced in PD patients, as compared to healthy participants. Furthermore, we show that PD patients under dopamine medication recover part of the brain-heart coupling, in proportion with the reduced motor symptoms. Our proposal offers a promising approach to unveil the physiopathology of PD and promoting the development of new diagnostic methods for the early stages of the disease.

Keywords

Parkinson’s disease, Brain-heart interaction, Network physiology, Dopamine, Interoception

Introduction

The understanding about the physiopathology and clinical phenotype of Parkinson's disease (PD) remains limited. PD is known to affect motor function, but non-motor symptoms such as autonomic dysfunction have a significant impact on patients' quality of life (*1*). Autonomic dysfunction can involve various bodily systems, including gastrointestinal, cardiovascular, urinary, erectile, thermoregulatory, and pupil contraction systems (*2*, *3*). Recent research shows that measuring brain-heart interactions can reveal the body's physiological state (*4*), which helps to diagnose and prognose brain-injured patients (*5–7*). Neurodegenerative diseases including PD may disrupt the awareness of one's own heartbeats, known as cardiac interoception, suggesting a disruption in the communication between the brain and the heart (*8–11*). Existing evidence of changes in the brain networks of PD patients (*12–14*), along with autonomic dysfunctions and disrupted interoception, lead to the hypothesis that PD patients may have altered brain-heart interactions.

In recent years, PD has been recognized as a condition that affects physiology at a network level, rather than just a focal brain region pathology (*15*, *16*). One of the physiological signatures of PD are the aberrant changes in brain connectivity, whose origin remains to be understood (*17*, *18*). We propose a new framework to study brain-heart interactions by quantifying the relationship between brain connectivity and estimators of cardiac sympathetic and parasympathetic activities. Our study cohort includes EEG and ECG 3 min resting state data from 16 healthy participants (HS, 7 males and 9 females, median age = 60.5±8 years) and 15 PD patients at an early state of the disease (7 males and 8 females, median age = 63± 8 years) (*19*). This study compares PD patients on and off dopaminergic therapy, as dopaminergic therapy has been shown to improve patient outcomes (*20*), to determine if physiological changes triggered by dopamine medication are reflected in brain-heart interactions.

Results

We estimated cardiac sympathetic and parasympathetic activities through a method based on the geometry of the interbeat intervals distributions as depicted in Poincaré plots (*21*). To quantify brain connectivity, a first-order adaptive Markov process was used (*22*). This helped to derive a directed connectivity measure between the fluctuations in power of two EEG channels at a defined frequency band, as shown in Figure 1. Maximal Information Coefficient (MIC) was used to quantify the linear and nonlinear couplings between the brain and the heartbeat-derived time series, resulting in an index in the range 0-1 (*23*). Statistical comparisons were based on finding clustered effects (*24*) on the brain-heart coupling measures (MIC values), between healthy participants and PD patients, and between PD on and off dopaminergic therapy.

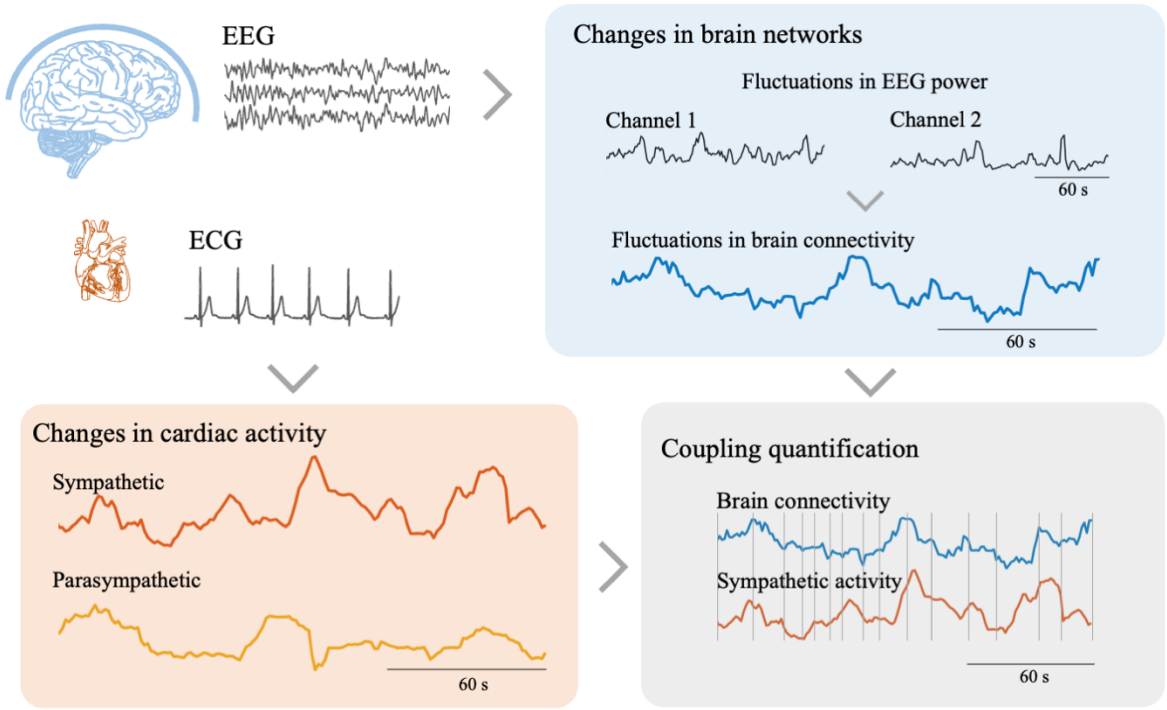

Figure 1. Methodological pipeline. (i) Computation of time-varying EEG power at different frequency bands (α, β, γ) and the estimation of time-varying connectivity between two EEG channels. (ii) Computation of the heart rate variability series from ECG and the estimation of cardiac sympathetic-parasympathetic activity. (iii) Brain connectivity-cardiac coupling estimation by computing the Maximal Information Coefficient (MIC). The coupling quantification is achieved by assessing the similarities between two time series, regardless of the curvature of the signals. The MIC method evaluates similarities between distinct segments individually, using an adjusted grid as depicted in the figure. The overall measure combines the similarities observed throughout the entire time-course.

We observed significant variations in the relationship between the brain connectivity and heartbeat dynamics among PD patients and healthy individuals. In healthy individuals, we observed a coupling between fluctuations in EEG connectivity and variations in cardiac dynamics. However, this coupling was weaker in PD patients, particularly in the relationship between slow fluctuations of heart rate variability (which are associated with sympathetic activity) and alpha and gamma connectivity.

We found differences when comparing the brain-heart coupling of healthy participants with that of PD patients who were not receiving dopaminergic therapy (PD off). Through cluster-based permutation tests, applied to the ensemble of EEG connectivity values coupled

with heartbeat dynamics, we discovered that one network in the alpha band was significantly linked to cardiac sympathetic indices, whose coupling was reduced in PD (Figure 2A and B, cluster statistics HS vs PD off, p = 0.0002, Z = 2.9844, cluster size = 154). These findings indicate that the resting state neural dynamics in PD are disturbed, affecting the interactions between brain connectivity and heartbeat dynamics. Importantly, these differences can be identified using non-invasive methods, without requiring any form of stimulation.

Dopaminergic therapy has been found to improve the reduced brain-heart coupling in patients with PD. This suggests that measures of brain-heart coupling are sensitive to the physiological changes induced by dopaminergic therapy in PD patients. We found a correlation between the brain-heart coupling and the changes in the motor evaluation in PD patients (as evaluated in the motor section of the Unified Parkinson's Disease Rating Scale–UPDRS III (*25*)). Specifically, the significant correlation between the improvement in motor symptoms and brain-heart coupling was found in the alpha band (Figure 2C, Spearman correlation, R = 0.6470, p = 0.0091).

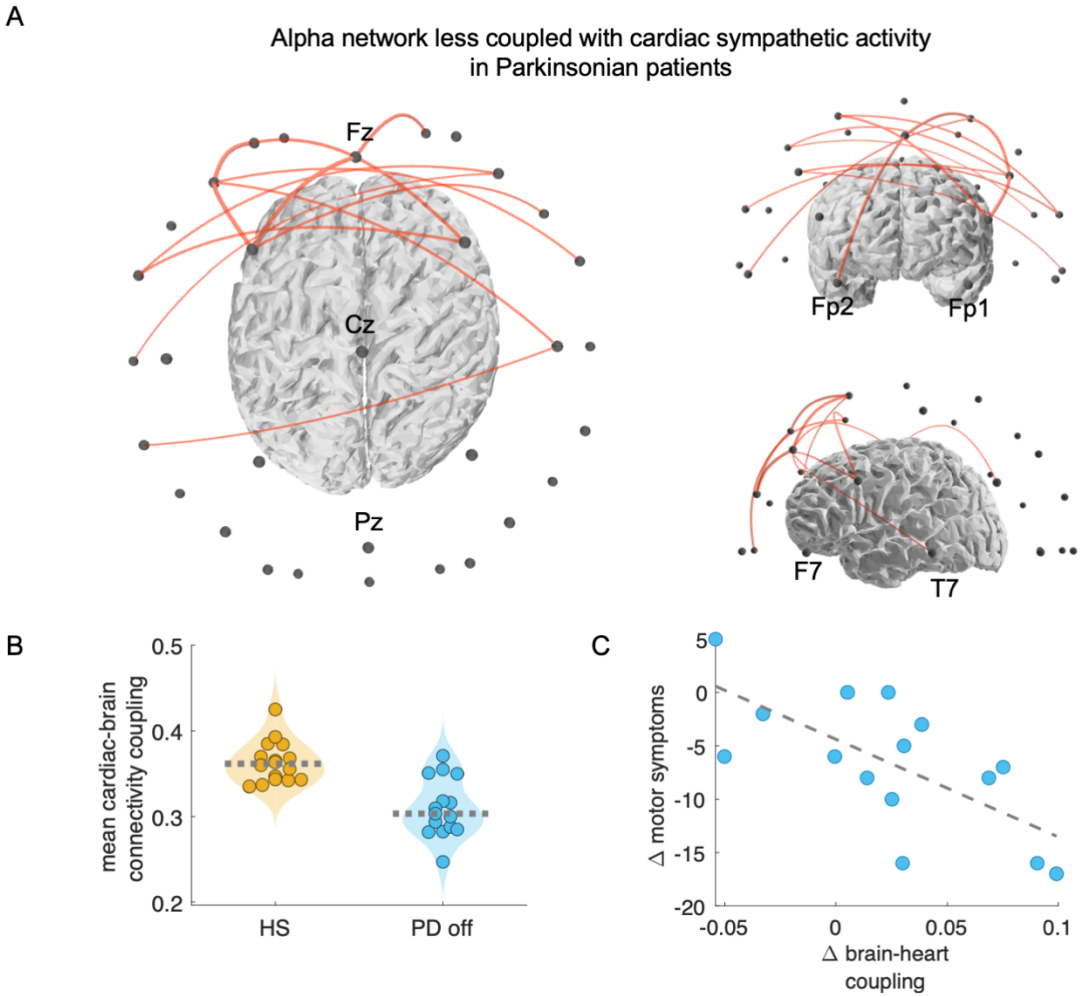

Figure 2. Significant alpha network that changed their coupling with cardiac sympathetic indices. (A) The network distinguishing healthy participants from PD patients off dopaminergic therapy. (B) Distribution of the mean brain-heart coupling. The dashed lines indicate the group medians. (C) Correlation between the changes in the brain-heart coupling (Δbrain-heart coupling, i.e., on minus off) and the changes in motor symptoms (motor section of the United Parkinson's Disease Rating Scale—where a lower score means better motor outcome). All values are in arbitrary units.

Additionally, we found two networks in the gamma band that were also linked to the estimation of cardiac sympathetic indices as well. These two networks were located in the

parieto-frontal (Cluster statistics HS vs PD off, $p < 0.0001$, $Z = 2.9844$, cluster size = 789) and parieto-temporal regions (Cluster statistics HS vs PD off, $p < 0.0001$, $Z = 2.7472$, cluster size = 398), as shown in Figure 3. These couplings showed no correlation with changes in motor symptoms in either gamma network 1 (Spearman correlation, $R = 0.4050$, $p = 0.1342$), or in gamma network 2 (Spearman correlation, $R = 0.4444$, $p = 0.0969$).

We found non-significant differences when comparing the mean connectivity values in the identified alpha network (Wilcoxon test, HS vs PD on, $p = 0.4177$; HS vs PD off, $p = 0.5936$; PD on vs PD off, $p = 0.1914$), gamma network 1 (Wilcoxon test, HS vs PD on, $p = 1$; HS vs PD off, $p = 0.3328$; PD on vs PD off, $p = 0.3066$) and gamma network 2 (Wilcoxon test, HS vs PD on, $p = 0.0930$; HS vs PD off, $p = 0.1184$; PD on vs PD off, $p = 0.8647$), cardiac sympathetic (Wilcoxon test, HS vs PD on, $p = 0.2436$; HS vs PD off, $p = 0.5143$; PD on vs PD off, $p = 0.8682$) and cardiac parasympathetic (Wilcoxon test, HS vs PD on, $p = 0.8279$; HS vs PD off, $p = 0.3954$; PD on vs PD off, $p = 0.2998$).

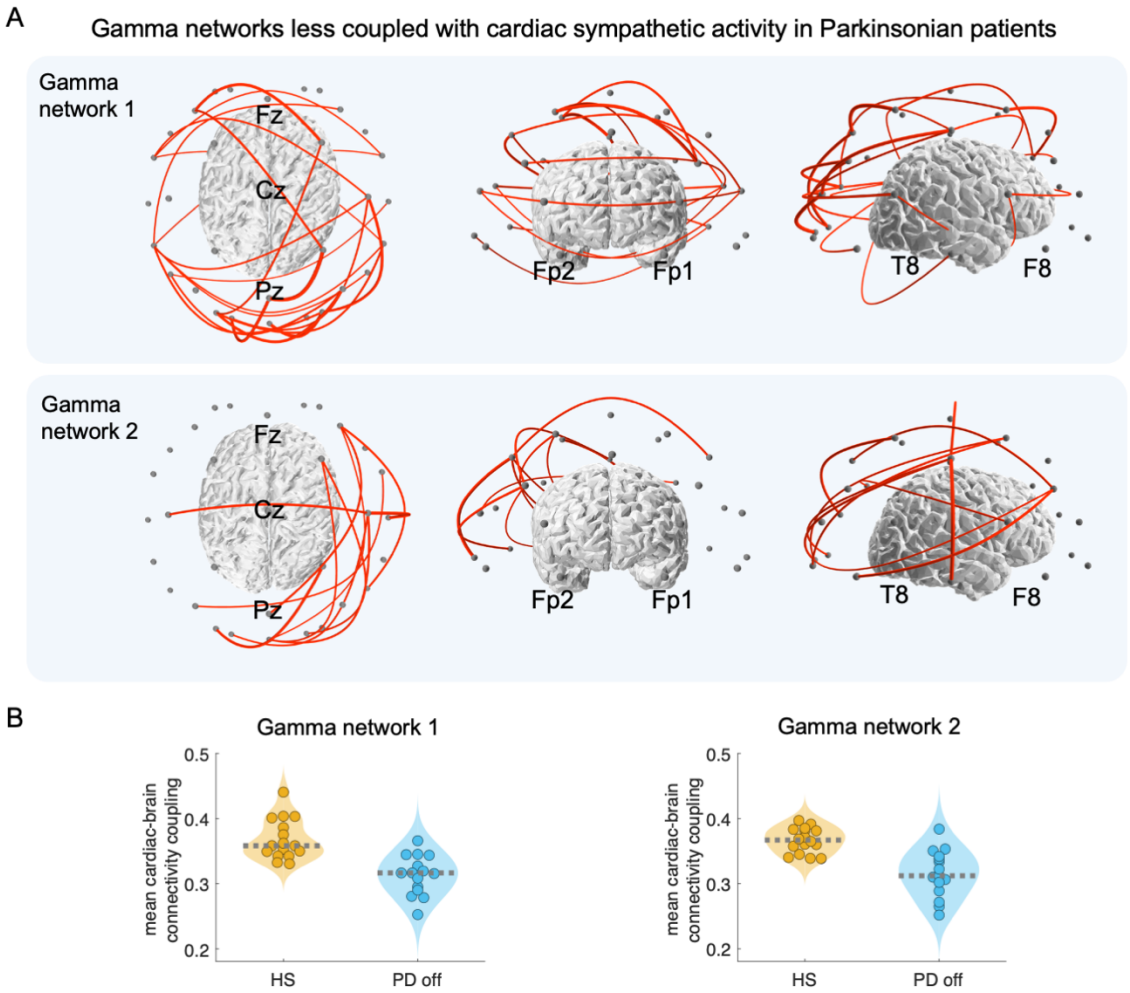

Figure 3. Significant gamma networks that changed their coupling with cardiac sympathetic indices. (A) The networks distinguishing healthy participants from PD patients off dopaminergic therapy. (B) Distribution of the mean brain-heart coupling. The dashed lines indicate the group medians. All values are in arbitrary units.

Furthermore, we examined the relationship between the brain and heartbeats by analyzing heartbeat-evoked responses (HERs), acknowledged markers of the central processing of cardiac inputs (*26*). HERs were gathered from the average of EEG epochs synchronized with the cardiac cycle. We compared HERs in healthy individuals to those with PD, both on and off dopaminergic therapy, and compared HERs in PD patients on and off dopamine therapy. Our

findings revealed distinct HER patterns when comparing PD patients on and off dopaminergic therapy (Cluster statistics PD on vs PD off. Positive clusters: $p_1 = 0.0008$, $Z_1 = 3.2942$; $p_2 = 0.0068$, $Z_2 = 3.0102$. Negative cluster: $p = 0.0037$, $Z = 2.8966$), as shown in Figure 4. However, there was only a slight difference between the two conditions, suggesting that higher-order brain-heart interaction analysis, such as the coupling between cardiac and brain networks may be a more suitable approach for characterizing PD.

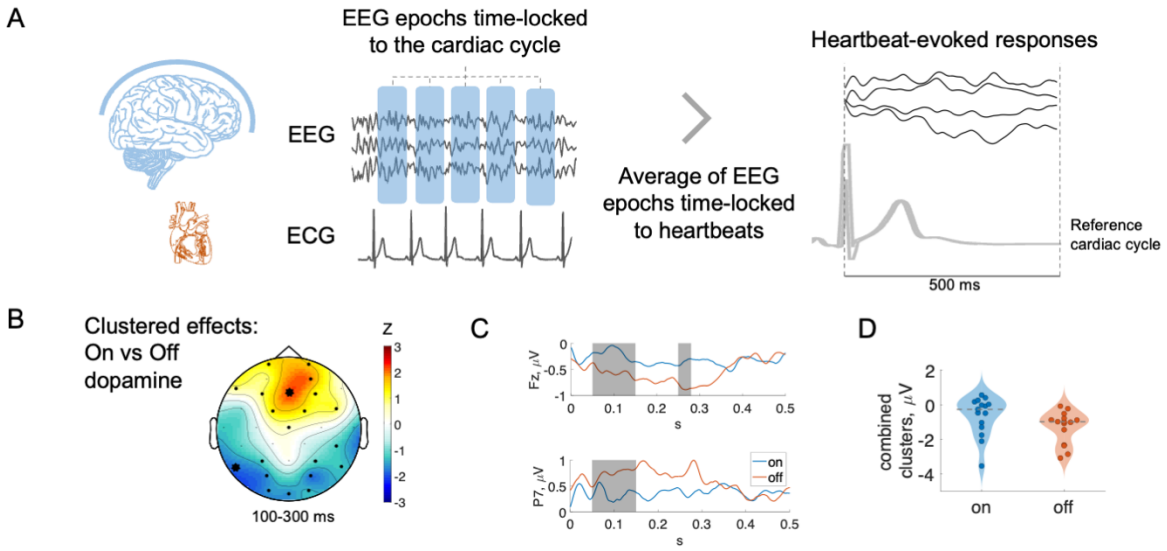

Figure 4. Heartbeat-evoked responses (HERs). (A) Pipeline to compute HERs. (B) Clustered effects found when comparing PD on vs PD off. Thick channels show clustered effects, and the color bar indicates the Z-value obtained from the paired Wilcoxon test. (C) Group median time course of the thick electrodes shown in (A). (D) Combined clustered effects.
PD on: Parkinsonian on dopamine, PD off: Parkinsonian off dopamine.

Discussion

The physiological basis of disrupted cardiac interoceptive pathways in PD, as assessed by brain-heart interactions, has not been significantly explored to date. Peripheral autonomic neurons are affected as well in PD (*27*), leading to symptoms of dysautonomia ranging among cardiovascular, respiratory, gastrointestinal, urinary, erectile, thermoregulatory, and pupil contraction disorders (*2*, *3*). The appearance of autonomic damage in PD has led to a search for specific abnormalities in autonomic function, e.g., heart rate variability (*28*, *29*), that could predict the disease. The reliability of these biomarkers remains uncertain due to the lack of understanding regarding their underlying mechanisms (*30*). Furthermore, the strongest evidence indicates that autonomic markers may rather provide insights into the severity and prognosis of PD (*31*).

The exploration of the relationship between brain connectivity and cardiac dynamics in PD is motivated by the substantial evidence of abnormal brain connectivity and autonomic abnormalities found in PD patients. These findings may provide a link to the observed disruptions in interoception in these individuals (*8–11*). Nigrostriatal fiber degeneration in PD disrupts the striato-cortical functional connectivity networks, leading to the known impairments in motor control (*32*). However, in the early stages of PD, changes in brain metabolism occur in key nodes of motor and cognitive networks, which can lead to disruptions in the connectivity of several regions (*33*, *34*). This has motivated the study of PD in terms of network-level phenomena rather than focal pathology (*15*, *16*). We investigated how cortical connectivity and heart rate variability covary at resting state. Our study found notable differences between the coupling between cardiac dynamics and brain connectivity in patients with PD and healthy individuals. In healthy participants, we noticed that changes in time-varying EEG connectivity are linked to changes in cardiac dynamics. However, this coupling is reduced in PD patients, especially in the connection between slow fluctuations of heart rate variability (considered predominantly sympathetic) and alpha and gamma connectivity. When PD patients are under dopaminergic therapy, the brain-heart coupling changes, suggesting a close link between the changes triggered by dopamine replacement and brain-heart coupling measures. This may indicate that markers of brain-heart interactions can capture dopaminergic-dependent mechanisms that are disrupted in PD. Indeed, one of the pathways affected by PD is the locus coeruleus-noradrenaline pathway (*35*). The disruptions in the locus coeruleus-noradrenaline pathway lead to changes in the slow fluctuations of heart rate variability, which are caused by changes in sympathetic activity resulting from variations in the noradrenaline release rate (*36*).

The acknowledged multi-organ dysfunction found in PD indicate that the physiopathology involves the disruption of several interoceptive pathways (*2*, *3*), including cardiac sympathetic denervation caused by the loss of catecholamine innervation in the nigrostriatal system and in the sympathetic nervous system (*37*). Previous behavioral studies have found that patients with PD have difficulty sensing their own heartbeats, namely cardiac interoception (*8*, *10*). This suggests that their brain-heart communication may be disrupted. In another study (*9*) the authors found an improved emotion recognition when healthy individuals performed an emotion recognition task after completing a cardiac interoception task. However, this effect was not observed in patients with PD (*9*). Furthermore, early PD has reported atrophy of the insula, key structure in interoceptive processing (*38*). Interoceptive inputs have been recognized as playing an important role in perception within computational frameworks of predictive coding (*39*) and consciousness (*4*), where dopamine is thought to be critical for processing interoceptive prediction errors (*40*, *41*). Numerous studies have shown that dopamine encodes learning and reward prediction (*42–45*), further supporting this idea. On account of the key role of dopamine-modulated mechanisms, it has been hypothesized that

dopamine participates in adaptation processes in predictive coding (*46*), which may extend to the role of dopamine in the regulation of the subjective experience of perception (*47*).

Our results may provide new insights for the understanding of the well-known abnormalities in brain connectivity of PD. For instance, PD patients show decreased connectivity in the supplementary motor area, dorsal lateral prefrontal cortex, and putamen, but increased connectivity in the cerebellum, primary motor cortex, and parietal cortex (*48*). PD patients may have higher connectedness within the sensorimotor and visual networks (*49*), due to compensation or loss of mutual inhibition between brain networks. Dopamine medication can normalize some patterns of functional connectivity, but the recovery level may depend on disease severity (*48*, *50*). In our results we observed a decrease in the coupling of cardiac sympathetic activity with brain connectivity measured in the alpha and gamma bands. EEG studies have revealed significant changes in the alpha-gamma range in PD, with reduced connectivity in alpha-beta bands and increased connectivity in the gamma band (*12*), but also aberrant cortical synchronization in the beta band (*17*, *18*). It remains to be confirmed whether our results relate to the repeatedly reported changes in brain connectivity in PD, including subcortical structures.

One of the believed causes of PD is the alpha-synuclein accumulation, is associated with neuronal death and synapse loss, as well as Lewy body formation. Noteworthy, these mechanisms affect dopamine transporter activity (*51*) and all the components of the central autonomic network, including cortical, insular, hypothalamic, brain stem, and spinal cord, as well as in peripheral structures like the vagus nerve, sympathetic nerve fibers, and enteric neural plexus (*52*). It remains to be explored whether the disrupted brain-heart interactions measured can be used as biomarkers of the early appearance of alpha-synuclein, or the migration of alpha-synuclein from peripheral systems to the brain (*53*, *54*), but also for the early PD diagnosis and the prognosis of cognitive and motor deficits (*55*).

Conclusions

The interactions between brain connectivity and cardiac dynamics can help us to better understand the complex physiopathology of PD, even in the early stages of the disease. We showed that cardiac sympathetic dynamics have a reduced coupling with brain connectivity patterns. Our results suggest a direct link between the already described changes in brain connectivity and autonomic dysfunctions in PD, which are potentially dopaminergic-dependent. We have demonstrated the potential of the study of brain-heart interactions in PD patients, whose exploitation may bring with advances in early diagnosis and the development of tools to be utilized in easily accessible clinical setups. Overall, our findings could inspire the development of new methods to investigate central nervous system and autonomic activity in both healthy individuals and those with pathological conditions.

Materials and methods

Dataset description

The dataset (*19*, *56*) includes 15 PD patients (7 males and 8 females, median age = 63± 8 years) and 16 healthy participants (7 males and 9 females, median age = 60.5±8 years). The median disease duration is 3±2 years (range 1 to 12 years). PD patients were diagnosed by a movement disorder specialist at Scripps clinic in La Jolla, California. Dopaminergic medication significantly improved motor symptoms, as measured by the motor section of the Unified Parkinson's Disease Rating Scale–UPDRS III (*25*), as performed in a paired Wilcoxon test ($Z = 2.9388$, $p = 0.0033$). Participants were right-handed and provided written consent in accordance with the Institutional Review Board of the University of California, San Diego, and the Declaration of Helsinki. Details on the demographic information of each participant are available in the original studies from this cohort (*19*, *56*).

PD patients' data were collected under on- and off-medication. On- and off-medication conditions were collected on different days with a counterbalanced order. For the on-medication recordings, patients continued their typical medication regimen. For the off-medication state, patients discontinued medication use at least 12 h before the session.

EEG data were acquired using a 32-channel BioSemi ActiveTwo system, together with a one-lead ECG, sampled at 512 Hz at rest for approximately 3 min.

EEG processing

EEG data were pre-processed using MATLAB R2022b and Fieldtrip Toolbox (*57*). Data were bandpass filtered with a fourth-order Butterworth filter, between 0.5 and 45 Hz. Large movement artifacts were removed using the wavelet-enhanced independent component analysis (*58*). Consecutively, an Independent Component Analysis (ICA) was re-run to identify and set to zero the components with eye movements and cardiac-field artifacts. To this end, one lead ECG was included as an additional input to the ICA to enhance the process of finding cardiac artifacts. Once the ICA components with eye movements and cardiac artifacts were visually identified, they were set to zero to reconstruct the EEG series. The results of this step were eye-movements and cardiac-artifact-free EEG data. Channels were re-referenced using a common average (*59*).

ECG processing

ECG time series were bandpass filtered using a fourth-order Butterworth filter, between 0.5 and 45 Hz. The R-peaks from the QRS waves were identified with an automatized process, followed by a visual inspection of misdetections. The procedure was based on a template-based method for detecting R-peaks (*59*). All the detected peaks were visually inspected over the original ECG, along with the inter-beat intervals histogram. Manual corrections of misdetections were performed if needed.

Computation of cardiac sympathetic and parasympathetic indices

The cardiac sympathetic and parasympathetic activities were estimated through a method based on the time-varying geometry of the interbeat interval (IBI) Poincaré plot (*21*). Poincaré plot is a non-linear method to study heart rate variability and depicts the fluctuations on the duration of consecutive IBIs (*60*). The features quantified from Poincaré plot are the SD_1 and SD_2, the ratios of the ellipse formed from consecutive changes in IBIs, representing the short- and long-term fluctuations of heart rate variability, respectively (*61*).

The ellipse ratios for the whole experimental condition SD_{01} and SD_{02} are computed as follows:

$$SD_{01} = \sqrt{\frac{1}{2}\, std(IBI')^2} \quad (1)$$

$$SD_{02} = \sqrt{2\, std(IBI)^2 - \frac{1}{2}\, std(IBI')^2} \quad (2)$$

where IBI' is the derivative of IBI and std() refers to the standard deviation.

The fluctuations of the ellipse ratios are computed with a sliding-time window, as shown in Eq. ***Erreur ! Source du renvoi introuvable.*** and ***Erreur ! Source du renvoi introuvable.***:

$$SD_1(t) = \sqrt{\frac{1}{2}\, std(IBI'_{\Omega_t})^2} \quad (3)$$

$$SD_2(t) = \sqrt{2\, std(IBI_{\Omega_t})^2 - \frac{1}{2}\, std(IBI'_{\Omega_t})^2} \quad (4)$$

where Ω_t: $t - T \leq t_i \leq t$, in this study T is fixed in 15 seconds.

The Cardiac Parasympathetic Index (CPI) and Cardiac Sympathetic Index (CSI) are computed as follows:

$$CPI(t) = SD_{01} + \overline{SD_1}(t) \quad (5)$$

$$CSI(t) = SD_{02} + \overline{SD_2}(t) \quad (6)$$

where $\overline{SD_x}$ is the demeaned SD_x

For a comprehensive description of the method, see (*21*).

EEG connectivity fluctuations

The EEG spectrogram was computed using the short-time Fourier transform with a Hanning taper. Calculations were performed through a sliding time window of 2 seconds with a 50% overlap, resulting in a spectrogram resolution of 1 second and 0.5 Hz. Time series were integrated within three frequency bands (alpha: 8-12 Hz, beta: 12-30 Hz, gamma: 30-45 Hz), based on previous EEG connectivity findings (*12*).

The directed time-varying connectivity between two EEG channels was quantified using an adaptative Markov process (*22*), as shown in Equation ***Erreur ! Source du renvoi introuvable.***, where *f* is the main frequency, θ_f is the phase ($f = 1, \ldots, 45$ *Hz)*. The model estimates the directed connectivity at a specific frequency band ($F = \{alpha, beta, gamma\}$) using least squares in a first order auto-regressive process with an external term, as shown in ***Erreur ! Source du renvoi introuvable.***, where A_F is a constant and ε_F is the adjusted error. Therefore, the directed connectivity is obtained from the adjusted coefficient from the external term B_F, as shown in Equation *(9)*.

$$EEG_{ch1}(t) = \sum_{f=f_1}^{f_n} a_f(t) \cdot sin(\omega_f\, t + \theta_f) \quad (7)$$

$$a_{F,ch1}(t) = A_F \cdot a_{F,ch1}(t\text{-}1) + B_F \cdot a_{F,ch2}(t\text{-}1) + \varepsilon_F, \quad (8)$$

$$C_{F,ch2\rightarrow ch1}(t) = B_F(t) \quad (9)$$

Brain-heart coupling estimation

The coupling between brain connectivity fluctuations and cardiac sympathetic-parasympathetic indices was assessed using Maximal Information Coefficient (MIC). MIC is a method that quantifies the coupling between two time series (*23*). MIC evaluates similarities between different segments separately at an adapted time scale that maximizes the mutual information, with a final measure that wraps the similarities across the whole time-course. The Equations *(10)* and *(11)* show the MIC computation between two time series X and Y. The mutual information I_g is computed to different grid combinations $g \in G_{xy}$. The mutual information values are normalized by the minimum joint entropy $\log_2 \min\{n_x, n_y\}$, resulting in an index in the range 0-1. Finally, the quantified coupling between X and Y corresponds to the normalized mutual information resulting from the grid that maximizes the MIC value.

$$\mathrm{m(X\,,\,Y)} = \frac{\max\limits_{g \in G_{xy}} I_g}{\log_2 \min\{n_x, n_y\}} \quad (10)$$

$$\mathrm{MIC(X\,,\,Y)} = \max_{n_x \times n_y < B} m(X, Y) \quad (11)$$

where $B = N^{0.6}$, and N is the dimension of the signals (*23*). The source code implementing MIC is available online at https://github.com/minepy.

The visualization of the brain networks coupled with heartbeat dynamics was performed using Vizaj (*62*).

Heartbeat-evoked responses analysis

Heartbeat-evoked responses (HERs) were defined by averaging time-locked EEG epochs with respect to R-peaks, from 0 to 500 ms (*63*). For HERs computation, the EEG epochs selection followed two rules: (i) epochs maximum absolute amplitude < 300 μV on any EEG channel, and (ii) the next heartbeat occurred at a latency later than 500 ms.

Statistical analysis

Statistical comparisons were based on Wilcoxon rank sum and signed rank tests, for unpaired and pared comparisons, respectively. P-values were corrected for multiple comparisons by using cluster-permutation analyses. Clustered effects were revealed using a non-parametric version of cluster permutation analysis (*24*). Cluster permutation analysis was applied to HERs and the MIC values computed between the directed connectivity and cardiac sympathetic/parasympathetic activity. Cluster-based permutation test included a preliminary mask definition, identification of candidate clusters and the computation of cluster statistics

with Monte Carlo's p-value correction. First, the preliminary mask was defined through Wilcoxon test, with alpha = 0.05, to the 992 MIC values corresponding to all the possible pair of channel combinations in both directions (Figure 5A). The identification of neighboring points was based on the default Biosemi neighborhood definition for 32 channels, and the neighboring connections were defined as shown in Figure 5B. A minimum cluster size of 5 neighbors was imposed. Cluster statistics were computed from 10,000 random partitions. The proportion of random partitions that resulted in a lower p-value than the observed one was considered as the Monte Carlo p-value, with significance at alpha = 0.05. The cluster statistic considered is the Wilcoxon's absolute maximum Z-value obtained from all the samples of the identified networks, separately (Figure 5C).

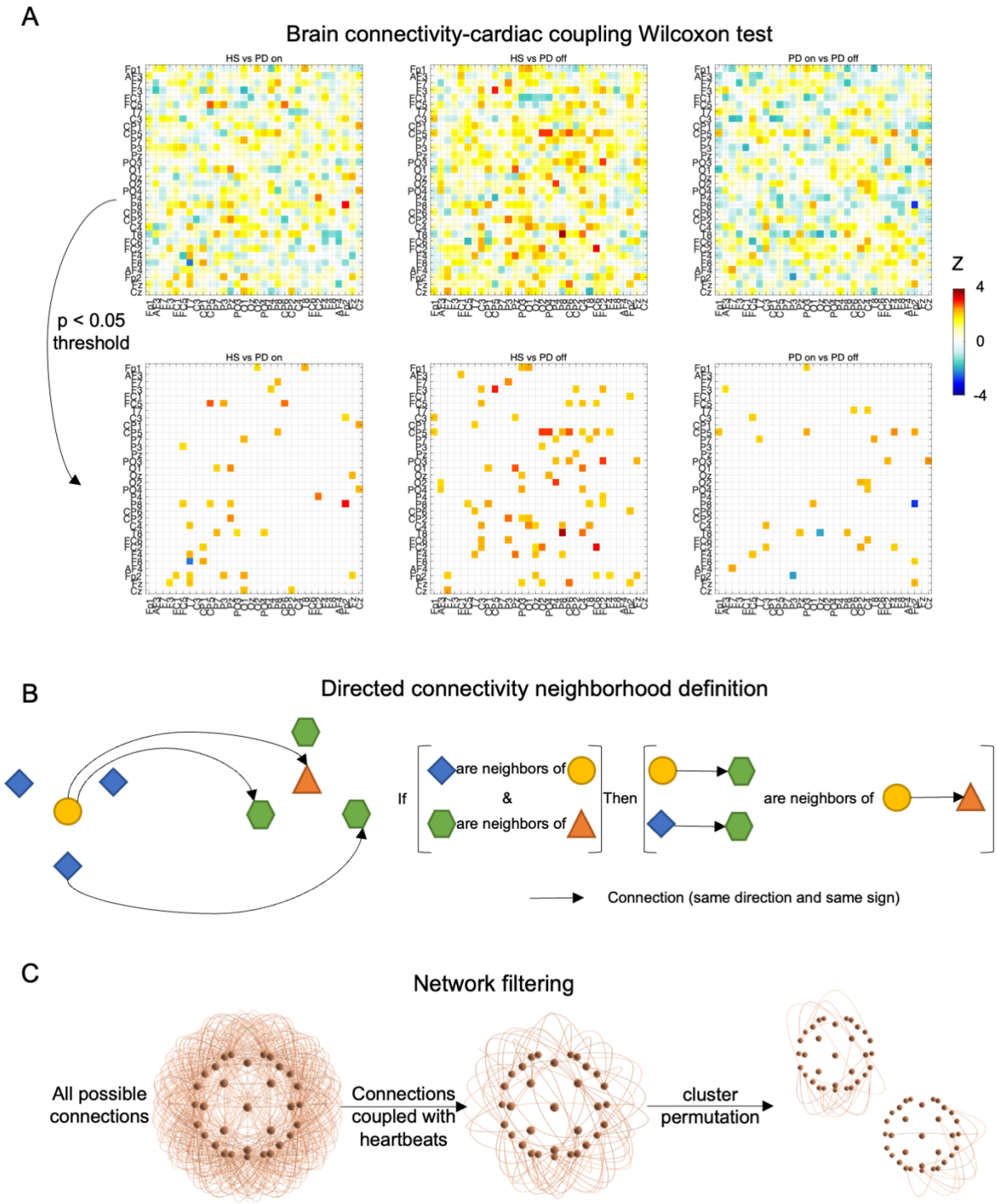

Figure 5. Network cluster permutation pipeline. (A) The connections that resulted in a p-value lower than the defined critical alpha are retained for constructing a preliminary mask for further analysis. (B) Neighboring connections are grouped by following the neighboring rule displayed. (C) Cluster statistics are computed for all the averaged connections that belong to the cluster and corrected for 10,000 permutations.

Resource availability

The data is part of a publicly available dataset "UC San Diego Resting State EEG Data from Patients with Parkinson's Disease", gathered from OpenNeuro.org the 21st of November of 2022 (*56*, *64*, *65*).

The utilized code come from different toolboxes for MATLAB. The functions for the computation of cardiac sympathetic and parasympathetic indices (*21*) are available at *https://github.com/diegocandiar/robust_hrv*. The functions for the computation of time-varying connectivity and brain-heart coupling are available at *https://github.com/diegocandiar/heart_brain_conn.* The functions for the computation of MIC values (*23*) are available at *https://github.com/minepy*. The functions to perform cluster permutation analyses (*24*) are available at *https://github.com/diegocandiar/eeg_cluster_wilcoxon.* The data analysis was performed using Fieldtrip toolbox (*57*), available at *https://github.com/fieldtrip/fieldtrip*

References

1. A. H. V. Schapira, K. R. Chaudhuri, P. Jenner, Non-motor features of Parkinson disease. *Nat Rev Neurosci*. **18**, 435–450 (2017).
2. S. Jain, Multi-organ autonomic dysfunction in Parkinson disease. *Parkinsonism & Related Disorders*. **17**, 77–83 (2011).
3. Y. Sharabi, G. D. Vatine, A. Ashkenazi, Parkinson's disease outside the brain: targeting the autonomic nervous system. *The Lancet Neurology*. **20**, 868–876 (2021).
4. D. Candia-Rivera, Brain-heart interactions in the neurobiology of consciousness. *Current Research in Neurobiology*. **3**, 100050 (2022).
5. B. Hermann, D. Candia-Rivera, T. Sharshar, M. Gavaret, J.-L. Diehl, A. Cariou, S. Benghanem, Aberrant brain-heart coupling is associated with the severity and prognosis of hypoxic-ischemic brain injury after cardiac arrest (2023), p. 2023.03.13.23287230, , doi:10.1101/2023.03.13.23287230.
6. D. Candia-Rivera, J. Annen, O. Gosseries, C. Martial, A. Thibaut, S. Laureys, C. Tallon-Baudry, Neural Responses to Heartbeats Detect Residual Signs of Consciousness during Resting State in Postcomatose Patients. *J. Neurosci.* **41**, 5251–5262 (2021).
7. D. Candia-Rivera, C. Machado, Multidimensional assessment of heartbeat-evoked responses in disorders of consciousness. *European Journal of Neuroscience* (2023), doi:10.1111/ejn.16079.
8. L. Ricciardi, G. Ferrazzano, B. Demartini, F. Morgante, R. Erro, C. Ganos, K. P. Bhatia, A. Berardelli, M. Edwards, Know thyself: Exploring interoceptive sensitivity in Parkinson's disease. *Journal of the Neurological Sciences*. **364**, 110–115 (2016).
9. P. C. Salamone, A. Legaz, L. Sedeño, S. Moguilner, M. Fraile-Vazquez, C. G. Campo, S. Fittipaldi, A. Yoris, M. Miranda, A. Birba, A. Galiani, S. Abrevaya, A. Neely, M. M. Caro, F. Alifano, R. Villagra, F. Anunziata, M. O. de Oliveira, R. M. Pautassi, A. Slachevsky, C. Serrano, A. M. García, A. Ibañez, Interoception Primes Emotional Processing: Multimodal Evidence from Neurodegeneration. *J. Neurosci.* **41**, 4276–4292 (2021).
10. G. Santangelo, C. Vitale, C. Baiano, A. D'Iorio, K. Longo, P. Barone, M. Amboni, M. Conson, Interoceptive processing deficit: A behavioral marker for subtyping Parkinson's disease. *Parkinsonism & Related Disorders*. **53**, 64–69 (2018).
11. J. L. Hazelton, S. Fittipaldi, M. Fraile-Vazquez, M. Sourty, A. Legaz, A. L. Hudson, I. G. Cordero, P. C. Salamone, A. Yoris, A. Ibañez, O. Piguet, F. Kumfor, Thinking versus feeling: How interoception and cognition influence emotion recognition in behavioural-variant frontotemporal dementia, Alzheimer's disease, and Parkinson's disease. *Cortex*. **163**, 66–79 (2023).
12. M. Conti, R. Bovenzi, E. Garasto, T. Schirinzi, F. Placidi, N. B. Mercuri, R. Cerroni, M. Pierantozzi, A. Stefani, Brain Functional Connectivity in de novo Parkinson's Disease Patients Based on Clinical EEG. *Frontiers in Neurology*. **13**, 844745 (2022).
13. S. Leviashvili, Y. Ezra, A. Droby, H. Ding, S. Groppa, A. Mirelman, M. Muthuraman, I. Maidan, EEG-Based Mapping of Resting-State Functional Brain Networks in Patients with Parkinson's Disease. *Biomimetics*. **7**, 231 (2022).
14. C. Hammond, H. Bergman, P. Brown, Pathological synchronization in Parkinson's disease: networks, models and treatments. *Trends in Neurosciences*. **30**, 357–364 (2007).
15. C. Gratton, J. M. Koller, W. Shannon, D. J. Greene, B. Maiti, A. Z. Snyder, S. E. Petersen, J. S. Perlmutter, M. C. Campbell, Emergent Functional Network Effects in Parkinson Disease. *Cerebral Cortex*. **29**, 2509–2523 (2019).
16. S. Wang, Y. Zhang, J. Lei, S. Guo, Investigation of sensorimotor dysfunction in Parkinson disease by resting-state fMRI. *Neuroscience Letters*. **742**, 135512 (2021).
17. N. Jackson, S. R. Cole, B. Voytek, N. C. Swann, Characteristics of Waveform Shape in

Parkinson's Disease Detected with Scalp Electroencephalography. *eNeuro*. **6**, 151–19 (2019).
18. N. C. Swann, C. de Hemptinne, A. R. Aron, J. L. Ostrem, R. T. Knight, P. A. Starr, Elevated synchrony in Parkinson disease detected with electroencephalography. *Ann Neurol*. **78**, 742–750 (2015).
19. J. S. George, J. Strunk, R. Mak-McCully, M. Houser, H. Poizner, A. R. Aron, Dopaminergic therapy in Parkinson's disease decreases cortical beta band coherence in the resting state and increases cortical beta band power during executive control. *NeuroImage: Clinical*. **3**, 261–270 (2013).
20. B. S. Connolly, A. E. Lang, Pharmacological Treatment of Parkinson Disease: A Review. *JAMA*. **311**, 1670–1683 (2014).
21. D. Candia-Rivera, Modeling brain-heart interactions from Poincaré plot-derived measures of sympathetic-vagal activity. *MethodsX*. **10**, 102116 (2023).
22. H. Al-Nashash, Y. Al-Assaf, J. Paul, N. Thakor, EEG signal modeling using adaptive Markov process amplitude. *IEEE Transactions on Biomedical Engineering*. **51**, 744–751 (2004).
23. D. N. Reshef, Y. A. Reshef, H. K. Finucane, S. R. Grossman, G. McVean, P. J. Turnbaugh, E. S. Lander, M. Mitzenmacher, P. C. Sabeti, Detecting Novel Associations in Large Datasets. *Science*. **334**, 1518–1524 (2011).
24. D. Candia-Rivera, G. Valenza, Cluster permutation analysis for EEG series based on non-parametric Wilcoxon–Mann–Whitney statistical tests. *SoftwareX*. **19**, 101170 (2022).
25. C. Ramaker, J. Marinus, A. M. Stiggelbout, B. J. van Hilten, Systematic evaluation of rating scales for impairment and disability in Parkinson's disease. *Movement Disorders*. **17**, 867–876 (2002).
26. H.-D. Park, O. Blanke, Heartbeat-evoked cortical responses: Underlying mechanisms, functional roles, and methodological considerations. *NeuroImage*. **197**, 502–511 (2019).
27. K. Wakabayashi, H. Takahashi, Neuropathology of Autonomic Nervous System in Parkinson's Disease. *ENE*. **38**, 2–7 (1997).
28. D. Devos, M. Kroumova, R. Bordet, H. Vodougnon, J. D. Guieu, C. Libersa, A. Destee, Heart rate variability and Parkinson's disease severity. *J Neural Transm*. **110**, 997–1011 (2003).
29. C.-A. Haensch, H. Lerch, J. Jörg, S. Isenmann, Cardiac denervation occurs independent of orthostatic hypotension and impaired heart rate variability in Parkinson's disease. *Parkinsonism & Related Disorders*. **15**, 134–137 (2009).
30. J.-A. Palma, H. Kaufmann, Autonomic disorders predicting Parkinson's disease. *Parkinsonism & Related Disorders*. **20**, S94–S98 (2014).
31. D. Brisinda, C. Sanchioni, R. Fenici, *European Heart Journal*, in press, doi:10.1093/eurheartj/ehab724.3043.
32. M. C. Ruppert, A. Greuel, M. Tahmasian, F. Schwartz, S. Stürmer, F. Maier, J. Hammes, M. Tittgemeyer, L. Timmermann, T. van Eimeren, A. Drzezga, C. Eggers, Network degeneration in Parkinson's disease: multimodal imaging of nigro-striato-cortical dysfunction. *Brain*. **143**, 944–959 (2020).
33. C. Huang, C. Tang, A. Feigin, M. Lesser, Y. Ma, M. Pourfar, V. Dhawan, D. Eidelberg, Changes in network activity with the progression of Parkinson's disease. *Brain*. **130**, 1834–1846 (2007).
34. S. Nigro, R. Riccelli, L. Passamonti, G. Arabia, M. Morelli, R. Nisticò, F. Novellino, M. Salsone, G. Barbagallo, A. Quattrone, Characterizing structural neural networks in de novo Parkinson disease patients using diffusion tensor imaging. *Hum Brain Mapp*. **37**, 4500–4510 (2016).
35. E. E. Benarroch, The locus ceruleus norepinephrine system: Functional organization and potential clinical significance. *Neurology*. **73**, 1699–1704 (2009).
36. H. Barcroft, H. Konzett, On the actions of noradrenaline, adrenaline and isopropyl

noradrenaline on the arterial blood pressure, heart rate and muscle blood flow in man. *J Physiol*. **110**, 194–204 (1949).
37. D. S. Goldstein, C. Holmes, S.-T. Li, S. Bruce, L. V. Metman, R. O. Cannon, Cardiac Sympathetic Denervation in Parkinson Disease. *Ann Intern Med*. **133**, 338–347 (2000).
38. D. O. Claassen, K. E. McDonell, M. Donahue, S. Rawal, S. A. Wylie, J. S. Neimat, H. Kang, P. Hedera, D. Zald, B. Landman, B. Dawant, S. Rane, Cortical asymmetry in Parkinson's disease: early susceptibility of the left hemisphere. *Brain and Behavior*. **6**, e00573 (2016).
39. F. H. Petzschner, S. N. Garfinkel, M. P. Paulus, C. Koch, S. S. Khalsa, Computational Models of Interoception and Body Regulation. *Trends in Neurosciences*. **44**, 63–76 (2021).
40. L. R. B. Spindler, A. I. Luppi, R. M. Adapa, M. M. Craig, P. Coppola, A. R. D. Peattie, A. E. Manktelow, P. Finoia, B. J. Sahakian, G. B. Williams, J. Allanson, J. D. Pickard, D. K. Menon, E. A. Stamatakis, Dopaminergic brainstem disconnection is common to pharmacological and pathological consciousness perturbation. *Proceedings of the National Academy of Sciences*. **118**, e2026289118 (2021).
41. A. K. Seth, K. Suzuki, H. D. Critchley, An interoceptive predictive coding model of conscious presence. *Front Psychol*. **2**, 395 (2011).
42. C. D. Fiorillo, P. N. Tobler, W. Schultz, Discrete Coding of Reward Probability and Uncertainty by Dopamine Neurons. *Science*. **299**, 1898–1902 (2003).
43. J. R. Hollerman, W. Schultz, Dopamine neurons report an error in the temporal prediction of reward during learning. *Nat Neurosci*. **1**, 304–309 (1998).
44. J. Mirenowicz, W. Schultz, Importance of unpredictability for reward responses in primate dopamine neurons. *Journal of Neurophysiology*. **72**, 1024–1027 (1994).
45. M. Pessiglione, B. Seymour, G. Flandin, R. J. Dolan, C. D. Frith, Dopamine-dependent prediction errors underpin reward-seeking behaviour in humans. *Nature*. **442**, 1042–1045 (2006).
46. P. R. Corlett, J. R. Taylor, X.-J. Wang, P. C. Fletcher, J. H. Krystal, Toward a neurobiology of delusions. *Progress in Neurobiology*. **92**, 345–369 (2010).
47. H. C. Lou, J. C. Skewes, K. R. Thomsen, M. Overgaard, H. C. Lau, K. Mouridsen, A. Roepstorff, Dopaminergic stimulation enhances confidence and accuracy in seeing rapidly presented words. *Journal of Vision*. **11**, 15 (2011).
48. T. Wu, L. Wang, Y. Chen, C. Zhao, K. Li, P. Chan, Changes of functional connectivity of the motor network in the resting state in Parkinson's disease. *Neuroscience Letters*. **460**, 6–10 (2009).
49. M. Göttlich, T. F. Münte, M. Heldmann, M. Kasten, J. Hagenah, U. M. Krämer, Altered Resting State Brain Networks in Parkinson's Disease. *PLOS ONE*. **8**, e77336 (2013).
50. T. van Eimeren, O. Monchi, B. Ballanger, A. P. Strafella, Dysfunction of the Default Mode Network in Parkinson Disease: A Functional Magnetic Resonance Imaging Study. *Archives of Neurology*. **66**, 877–883 (2009).
51. C. Wersinger, A. Sidhu, Attenuation of dopamine transporter activity by α-synuclein. *Neuroscience Letters*. **340**, 189–192 (2003).
52. Z. Chen, G. Li, J. Liu, Autonomic dysfunction in Parkinson's disease: Implications for pathophysiology, diagnosis, and treatment. *Neurobiology of Disease*. **134**, 104700 (2020).
53. C. Challis, A. Hori, T. R. Sampson, B. B. Yoo, R. C. Challis, A. M. Hamilton, S. K. Mazmanian, L. A. Volpicelli-Daley, V. Gradinaru, Gut-seeded α-synuclein fibrils promote gut dysfunction and brain pathology specifically in aged mice. *Nat Neurosci*. **23**, 327–336 (2020).
54. S. Kim, S.-H. Kwon, T.-I. Kam, N. Panicker, S. S. Karuppagounder, S. Lee, J. H. Lee, W. R. Kim, M. Kook, C. A. Foss, C. Shen, H. Lee, S. Kulkarni, P. J. Pasricha, G. Lee, M. G. Pomper, V. L. Dawson, T. M. Dawson, H. S. Ko, Transneuronal Propagation of Pathologic α-Synuclein from the Gut to the Brain Models Parkinson's Disease. *Neuron*. **103**, 627-641.e7 (2019).

55. T. Eckert, C. Tang, D. Eidelberg, Assessment of the progression of Parkinson's disease: a metabolic network approach. *The Lancet Neurology*. **6**, 926–932 (2007).
56. A. P. Rockhill, N. Jackson, J. S. George, A. R. Aron, N. C. Swann, UC San Diego Resting State EEG Data from Patients with Parkinson's Disease. *OpenNeuro [Dataset]* (2021), doi:10.18112/openneuro.ds002778.v1.0.5.
57. R. Oostenveld, P. Fries, E. Maris, J.-M. Schoffelen, *Computational Intelligence and Neuroscience*, in press, doi:10.1155/2011/156869.
58. L. J. Gabard-Durnam, A. S. Mendez Leal, C. L. Wilkinson, A. R. Levin, The Harvard Automated Processing Pipeline for Electroencephalography (HAPPE): Standardized Processing Software for Developmental and High-Artifact Data. *Front. Neurosci.* **12**, 97 (2018).
59. D. Candia-Rivera, V. Catrambone, G. Valenza, The role of electroencephalography electrical reference in the assessment of functional brain–heart interplay: From methodology to user guidelines. *Journal of Neuroscience Methods*. **360**, 109269 (2021).
60. M. Brennan, M. Palaniswami, P. Kamen, Do existing measures of Poincare plot geometry reflect nonlinear features of heart rate variability? *IEEE Transactions on Biomedical Engineering*. **48**, 1342–1347 (2001).
61. R. Sassi, S. Cerutti, F. Lombardi, M. Malik, H. V. Huikuri, C.-K. Peng, G. Schmidt, Y. Yamamoto, D. Reviewers, B. Gorenek, G. Y. H. Lip, G. Grassi, G. Kudaiberdieva, J. P. Fisher, M. Zabel, R. Macfadyen, Advances in heart rate variability signal analysis: joint position statement by the e-Cardiology ESC Working Group and the European Heart Rhythm Association co-endorsed by the Asia Pacific Heart Rhythm Society. *Europace*. **17**, 1341–1353 (2015).
62. T. Rolland, F. D. V. Fallani, Vizaj—A free online interactive software for visualizing spatial networks. *PLOS ONE*. **18**, e0282181 (2023).
63. H.-D. Park, O. Blanke, Heartbeat-evoked cortical responses: Underlying mechanisms, functional roles, and methodological considerations. *NeuroImage*. **197**, 502–511 (2019).
64. S. Appelhoff, M. Sanderson, T. L. Brooks, M. van Vliet, R. Quentin, C. Holdgraf, M. Chaumon, E. Mikulan, K. Tavabi, R. Höchenberger, D. Welke, C. Brunner, A. P. Rockhill, E. Larson, A. Gramfort, M. Jas, MNE-BIDS: Organizing electrophysiological data into the BIDS format and facilitating their analysis. *Journal of Open Source Software*. **4**, 1896 (2019).
65. C. R. Pernet, S. Appelhoff, K. J. Gorgolewski, G. Flandin, C. Phillips, A. Delorme, R. Oostenveld, EEG-BIDS, an extension to the brain imaging data structure for electroencephalography. *Sci Data*. **6**, 103 (2019).

Acknowledgements

Funding
Research supported by Agence Nationale de la Recherche (France), grant ANR-20-CE37-0012-03.

Author contributions
Conceptualization: DCR
Methodology: DCR
Visualization: DCR
Investigation: DCR, MV, MC, FDVF
Supervision: MC, FDVF
Writing – first version of the manuscript: DCR
Writing – review & editing: DCR, MV, MC, FDVF

Competing interests
The authors declare that they have no competing interests.